Lack of bystander activation shows that localization exterior to chromosome territories is not sufficient to up-regulate gene expression

Céline Morey,[1] Clémence Kress,[2] and Wendy A. Bickmore[3]

MRC Human Genetics Unit, Edinburgh EH4 2XU, Scotland, United Kingdom

Position within chromosome territories and localization at transcription factories are two facets of nuclear organization that have been associated with active gene expression. However, there is still debate about whether this organization is a cause or consequence of transcription. Here we induced looping out from chromosome territories (CTs), by the activation of *Hox* loci during differentiation, to investigate consequences on neighboring loci. We show that, even though flanking genes are caught up in the wave of nuclear reorganization, there is no effect on their expression. However, there is a differential organization of active and inactive alleles of these genes. Inactive alleles are preferentially retained within the CT, whereas actively transcribing alleles, and those associated with transcription factories, are found both inside and outside of the territory. We suggest that the alleles relocated further to the exterior of the CT are those that were already active and already associated with transcription factories before the induction of differentiation. Hence active gene regions may loop out from CTs because they are able to, and not because they need to in order to facilitate gene expression.

[Supplemental material is available online at www.genome.org.]

Gene organization along the primary DNA sequence of mammalian genomes is not random. Genes that, for the most part, are functionally unrelated, cluster in the genome and selection has acted to prevent these clusters from becoming fragmented during evolution (Singer et al. 2005). The genes in these clusters tend to be expressed at high levels (Caron et al. 2001) and/or in a wide range of tissues (Lercher et al. 2002). Moreover, reporter genes are also expressed at higher levels when inserted into these domains compared with other genomic regions (Gierman et al. 2007). It has been suggested that gene clustering facilitates transcriptional activation by creating regions of open decondensed chromatin (Sproul et al. 2005). Similarly, colocalization of active genes at focal concentrations of RNA polymerase II (transcription factories) or splicing factors (splicing speckles) may enhance the efficiency of gene expression (Shopland et al. 2003; Osborne et al. 2004; Fraser and Bickmore 2007; Brown et al. 2008). Indeed, nuclear clustering of gene-rich domains, both in *cis* and in *trans*, has been detected by diverse techniques (Shopland et al. 2006; Simonis et al. 2006). Many of these gene-rich domains have also been seen to adopt positions at the edge or outside of chromosome territories (CTs)—termed looping out, but regardless of the activity of individual genes within them (Mahy et al. 2002; Brown et al. 2006). Hence, it remains unclear whether there is a causal relationship between CT reorganization and transcription. In one case, an increased frequency of looping out, induced by the insertion of a beta-globin LCR, did accompany increased association of the flanking genes with transcription factories and an activation of some gene expression (Noordermeer et al. 2008).

Present addresses: [1]Institut Pasteur, Roux 75015, Paris, France; [2]Institut National de la Recherche Agronomique, 78352 Jouy-en-Josas Cedex, France.
[3]Corresponding author.
E-mail W.Bickmore@hgu.mrc.ac.uk; fax 44-131-467-8456.
Article published online before print. Article and publication date are at http://www.genome.org/cgi/doi/10.1101/gr.089045.108.

Gene clusters where intra-CT organization most closely correlates with expression are those that contain functionally related and coregulated genes. When silent, these clusters, which are mainly located inside of CTs, upon induction of expression will relocate more toward the outside of CTs (Volpi et al. 2000; Williams et al. 2002). Examples of such gene clusters are the murine *Hoxb* and *Hoxd* loci. CT reorganization accompanies their induction, both during the differentiation of embryonic stem (ES) cells and also along the anterior–posterior axis of the developing embryo (Chambeyron and Bickmore 2004; Chambeyron et al. 2005; Morey et al. 2007). However, the absence of looping out of *Hoxd* from its CT in the limb bud (Morey et al. 2007), and the ability of a transposed *Hoxb1* to induce some looping out in the absence of transcription (Morey et al. 2008), question the absolute requirement for this facet of nuclear reorganization in promoting gene expression.

Paralogous mammalian *Hox* loci evolved by duplication of an ancestral cluster during vertebrate radiation (Ferrier and Minguillon 2003). The apparent similarity in the nuclear behavior of *Hoxb* and *Hoxd* occurs despite the very different genomic contexts within which they are found. *Hoxd* is within an extensive gene desert. Aside from the closely linked *Mtx2, Evx2*, and *Lnp*, there are no other annotated genes for 600–700 kilobases (kb) 3′ or 5′ of *Hoxd*. In contrast, *Hoxb* is embedded in a gene-dense region, flanked by many unrelated genes (Fig. 1). This raises interesting questions as to how genomic environments impact the expression and nuclear organization of *Hox* loci and, conversely, how activation and reorganization of these *Hox* loci affects the flanking genes and genomic regions.

Using DNA-fluorescence in situ hybridization (FISH), coupled with gene expression analysis during ES cell differentiation, we show that intra-CT reorganization, initiated within *Hox* clusters, then spreads out for hundreds of kilobases into adjacent genomic regions that, in the case of *Hoxb*, contain many unrelated genes. We show that the expression of these flanking genes is not affected by their being swept up in extensive CT reorganization. Using

19:1184–1194 © 2009 by Cold Spring Harbor Laboratory Press; ISSN 1088-9051/09; www.genome.org

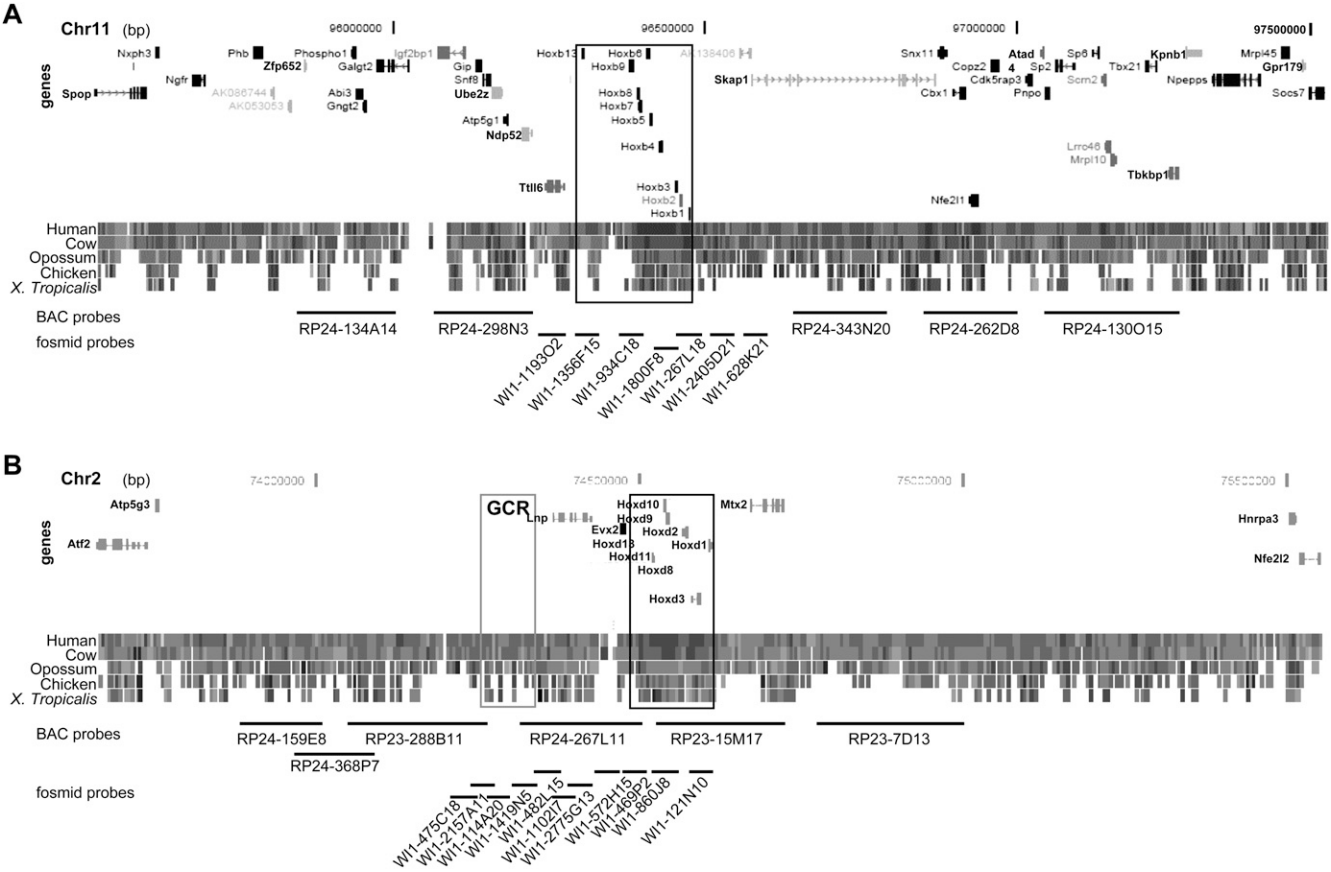

Figure 1. Comparative genomic structure of *Hoxb* and *Hoxd*. Map of the 2 Mb genomic regions surrounding *Hoxb* on MMU11 (*A*) and surrounding *Hoxd* on MMU2 (*B*) showing the position of genes, the level of conservation between the murine locus and other vertebrates, and the position of BACs and fosmids used as probes in this study (Supplemental Table S1). The *Hoxb* and *Hoxd* loci are boxed in black. The gray box locates a region of noncoding sequence conservation that includes the global control region (GCR). Data and map positions (bp) are taken from the August 2005 NCBI Build 35 of the mouse genome (http://genome.ucsc.edu/cgi-bin/hgGateway) and from Ensembl v37, February 2006 (http://www.ensembl.org/Mus_musculus/index.html).

RNA-FISH we show that inactive and active alleles of these flanking genes do differ in their intra-CT distribution, with inactive alleles preferentially retained within the CT. However, the actively transcribing alleles locate inside, at the edge, and outside of the CT. Similarly, by immuno-FISH we show that the association of gene loci with transcription factories is preferentially, but not exclusively, seen toward the edge and outside of the CT. The alleles that are relocated further to the exterior of the CT appear to be those that were already active and that were already associated with transcription factories. We suggest that silent *Hox* loci are restrained to localizations inside of CTs and that, upon their activation, a change in long-range chromatin structure releases this constraint. This then allows enough freedom of movement for the chromatin of a large genomic region, which includes not just the *Hox* loci but also flanking genes, to be able to now locate in many positions relative to the CT.

Results

Distinct nuclear behaviors of *Hoxb* and *Hoxd* regions in undifferentiated cells

In undifferentiated ES cells, silent *Hox* clusters are preferentially located at the edge or inside of their CTs (Chambeyron and Bickmore 2004; Morey et al. 2007). To determine if this is a feature intrinsic to *Hox* clusters themselves, or whether it is influenced by the flanking genomic regions, we used 2D FISH on nuclei of undifferentiated OS25 ES cells to measure the intra-CT position of signals from probe pairs covering >1 Mb around *Hoxb* and *Hoxd* (Figs. 1, 2A; Supplemental Table S1).

The whole *Hoxd* region, including flanking gene deserts, located well inside the MMU2 CT (≥60% alleles at distance >0.4 μm) with <15% of alleles found outside (Fig. 2B). A different picture was seen at *Hoxb* where, consistent with previous studies (Chambeyron and Bickmore 2004), significantly more loci (~30%) were seen outside of the respective CT than at *Hoxd* ($P < 10^{-3}$). This was especially pronounced at the 5′ end of the cluster and extends to the 5′ flanking region (>40% alleles <−0.2 μm).

This difference in nuclear organization between *Hoxb* and *Hoxd* may reflect the activity of the surrounding regions. To investigate this we hybridized cDNA from undifferentiated ES cells to a mouse 38K cDNA array (GEO accession: GSE15166) and to a custom tiling array for the *Hoxb* and *Hoxd* loci and their surrounding regions (Fig. 2C; Supplemental Table S2).

As previously assessed by RT-PCR (Chambeyron and Bickmore 2004; Chambeyron et al. 2005; Morey et al. 2007), *Hoxb* and *Hoxd* genes were expressed either very weakly, or not at all. In contrast, high steady-state levels of transcripts were detected for some genes 5′ (*Igf2bp1*, *Snf8*, *Ube2z*, and *Ndp52*) and 3′ (*Nfe2l1*) of *Hoxb*.

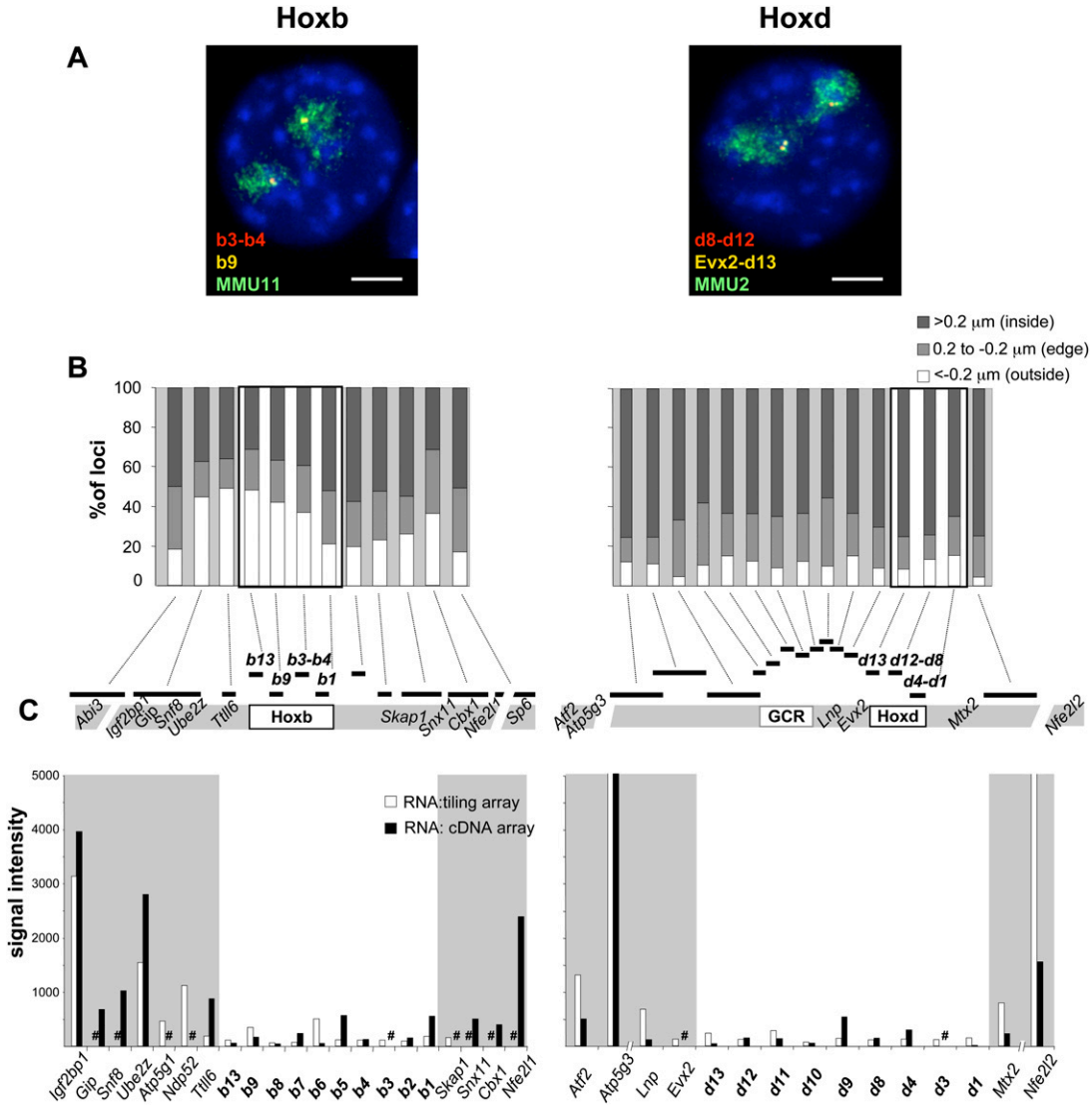

Figure 2. Nuclear organization and gene expression at *Hoxb* and *Hoxd* in undifferentiated ES cells. (*A*) Four-color DNA-FISH on DAPI counterstained nuclei from undifferentiated OS25 ES cells using; (*left* panel) fosmid probes WI1-1800F8 (b3-b4, red), WI1-934C18 (b9, yellow), and an MMU11 chromosome paint (green) and (*right* panel) fosmid probes WI1-860J8 (d8-d12, red), WI1-469P2 (Evx2-d13, yellow), and an MMU2 chromosome paint (green). Bar, 5 μm. (*B*) Percentage of *Hoxb* or *Hoxd* region signals located either inside (>0.2 μm; dark gray bars), at the edge (±0.2 μm; light gray bars) or outside (<−0.2 μm; white bars) of the respective CT edge. The location of the probes is depicted on the map *underneath* the histograms. A minimum of 50 nuclei/100 territories was analyzed. (C) Intensities of signals of cDNA from undifferentiated OS25 ES cells hybridized on a tiling microarray (white columns) or on a cDNA microarray (black columns). Combined results from three independent experiments, including a dye swap, are shown. A sharp sign indicates genes not represented on the respective array.

Hence, the differential CT organization of *Hoxb* and *Hoxd* before differentiation likely reflects the transcriptional activity of the genes flanking *Hoxb*.

Chromosome territory reorganization during ES cell differentiation extends out to the regions that surround *Hox* loci

When activated during ES cell differentiation, an increased frequency of *Hox* alleles are seen at positions outside of their CTs, as measured either by 2D FISH in differentiating ES cells, or by 3D FISH in differentiating ES cells and in the embryo proper (Chambeyron and Bickmore 2004; Chambeyron et al. 2005; Morey et al. 2007). To determine if this level of nuclear reorganization is restricted just to the *Hox* genes themselves, or whether it spreads further, we analyzed the position, relative to the CT edge, of hybridization signals from probes across the genomic regions, in ES cells that had been differentiated for 3 and 7 d (Fig. 3A,B). As previously reported (Chambeyron and Bickmore 2004), the most extensive looping out was seen at the early stages of differentiation (D3) and at the 3′ end of *Hoxb*. This decreased by day 7 and, at this time point, looping out had spread to the 5′ end of *Hoxb*. A significant relocalization further to the outside of the CT also spreads >500 kb 3′ of *Hoxb* into the flanking gene regions. No additional CT reorganization was detected for the 5′ flanking domain, which is already mainly located outside, or at the edge, of

the CT in undifferentiated cells. This was reconfirmed in 3D FISH of pFa-fixed cells (Fig. 3C). However, the absolute percentages of *Hoxb1*, *Igf2bp1*, or *Cbx1* signals located outside, or at the edge, of the CT during differentiation were lower than those measured by 2D FISH. This suggests that, as we have previously described (Morey et al. 2007), methanol/acetic acid fixation of 2D FISH exaggerates the nuclear movements compared to pFa fixation.

At *Hoxd*, CT reorganization also spreads 3′ over *Mtx2* and 5′ over *Lnp* (Fig. 3A,B; Morey et al. 2007). In the 5′ direction, FISH signals from all fosmids from WI1-1102I7 through to WI1-2157A11 (Fig. 1) showed significant movement toward the edge of the CT ($P < 0.05$) at D3 of differentiation (Fig. 3). However, there was no significant reorganization ($P = 0.165$) detected with the next clone—WI1-475C18. Intriguingly, this boundary to the spread of CT reorganization 5′ of *Hoxd* corresponds to the end of a long-range regulatory region termed the GCR. As at *Hoxb*, the extent of intra-CT reorganization of *Hoxd*, decreased by D7.

The spread of CT reorganization does not affect expression of flanking genes

To test whether the spreading of CT reorganization to the genomic regions flanking *Hox* clusters impacts the expression of genes located there, we analyzed gene expression after D3 of differentiation

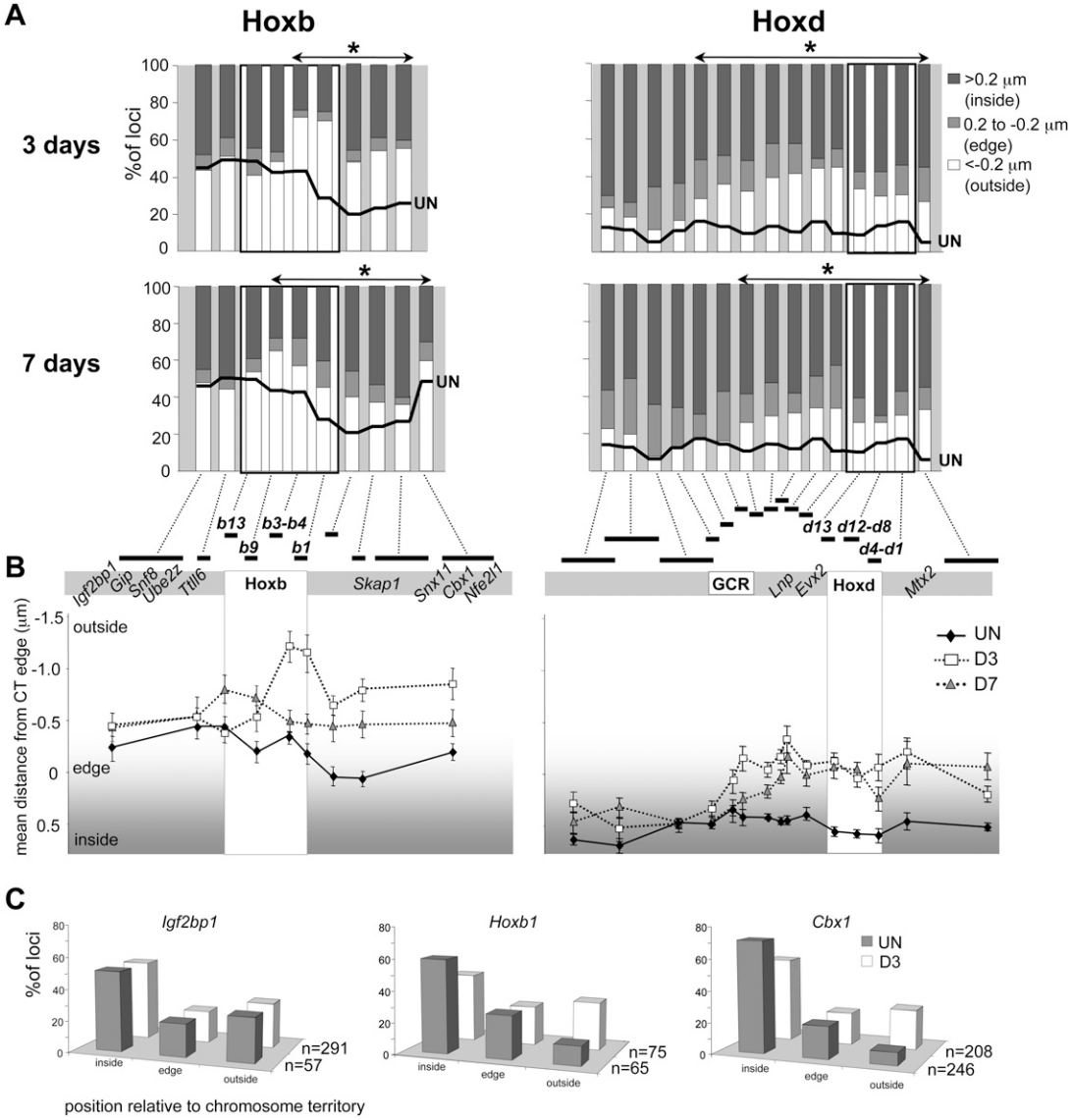

Figure 3. Chromosome territory reorganization during ES cell differentiation. (*A*) Histograms showing the percentage of signals across the *Hoxb* or *Hoxd* regions located on either inside (>0.2 μm; dark gray bars), at the edge (±0.2 μm; light gray bars), or outside (<−0.2 μm white bars) of the MMU11 (*Hoxb*) or the MMU2 CT (*Hoxd*), as measured by 2D FISH in OS25 ES cells differentiated for 3 or 7 d. The thick black line shows the corresponding data in undifferentiated ES cells (from Fig. 2B). Probes showing a further significant ($P < 0.05$) relocalization toward the outside of the CT during differentiation are indicated by the asterisked regions ($n = 100$). (*B*) Mean position (μm) ± SEM, measured by 2D FISH, of the *Hoxb* genomic region relative to the edge of MMU11 CT (*left*), or of the *Hoxd* genomic region relative to the edge of MMU2 CT (*right*) in undifferentiated OS25 ES cells (filled diamonds) and in cells differentiated for 3 d (open squares) or 7 d (shaded triangles). (*C*) Position of *Hoxb1* and 5′ (*Ifg2bp1*) or 3′ (*Cbx1*) flanking regions relative to the MMU11 CT (inside of, edge, or outside of) assayed by 3D FISH in pFa fixed undifferentiated ES cells (filled bars), and cells differentiated for 3 d (open bars).

(Fig. 4). Differentiation was apparent from the dramatically reduced steady-state levels of transcripts from three markers of pluripotency (*Oct4*, *Sox2,* and *Nanog*). mRNA levels of two constitutively expressed housekeeping genes, *Rrm2* and *Hprt1*, remained constant. There was strong induction of *Hoxb* genes during differentiation (Fig. 4B), and this was supported by RT-PCR data (not shown). In contrast, there was no detectable induction of neighboring genes on either side of *Hoxb*. Indeed, expression of *Skap1*, located immediately 3′ of *Hoxb1*, appeared to be decreased upon differentiation as judged from the tiling array (this gene is not present on the expression array used), even though this gene is significantly relocalized further toward the outside of the CT during differentiation (Fig. 3). In comparison with *Hoxb*, *Hoxd* genes are only moderately up-regulated during differentiation. This might be linked to the differentiation pathways the cells have engaged in, or the different genomic contexts of the two *Hox* clusters.

We conclude that there is no bystander activation of flanking unrelated genes during *Hox* gene induction, and that the enhanced looping out from the CT during *Hox* activation does not, de facto, lead to the activation of otherwise silent genes, nor does it further enhance the transcription of already active genes.

Hoxb and *Hoxd* are not colocalized in the nucleus

What then is the functional significance of looping out for the *Hox* genes themselves? One possibility is that *Hox* loci are being relocalized to a specific nuclear site to enable their coordinate regulation by shared regulatory complexes. There is conflicting data with regard to nuclear colocalization of *Hox* loci in *Drosophila* and whether this is related to their regulation by polycomb (PcG) complexes (Bantignies et al. 2003; Fedorova et al. 2008). Therefore, we analyzed the spatial proximity of *Hoxb1* and *Hoxd1* alleles in ES cells, before and after differentiation (Fig. 5A). Consistent with another study (Lanctot et al. 2007), we did not detect evidence for substantial colocalization, or close association, of *Hox* loci in *trans*, either in the silent (undifferentiated) or active (differentiated) state by 2D FISH (Fig. 5B). There was also no colocalization seen by 3D FISH of differentiated cells (Fig. 5C).

Preferential CT organization of nonexpressing vs. expressing alleles

To more directly address the relationship between gene expression and CT organization we determined the nuclear distribution of transcribing alleles using RNA-FISH with intron probes (Supplemental Table S3) followed by DNA-FISH with genomic probes. We were unable to visualize nascent RNA signals for *Hoxb1* or *Hoxd1*, probably due to the short and single intron structure of their transcription units, thus ensuring rapid mRNA processing and export to the cytoplasm. Therefore, we analyzed the nuclear behavior of two constitutively expressed genes, *Igf2bp1* and *Cbx1*, which flank *Hoxb* to the 5′ and 3′ sides, respectively (Fig. 1). *Igf2bp1* is in a region that is already substantially (35% of alleles)

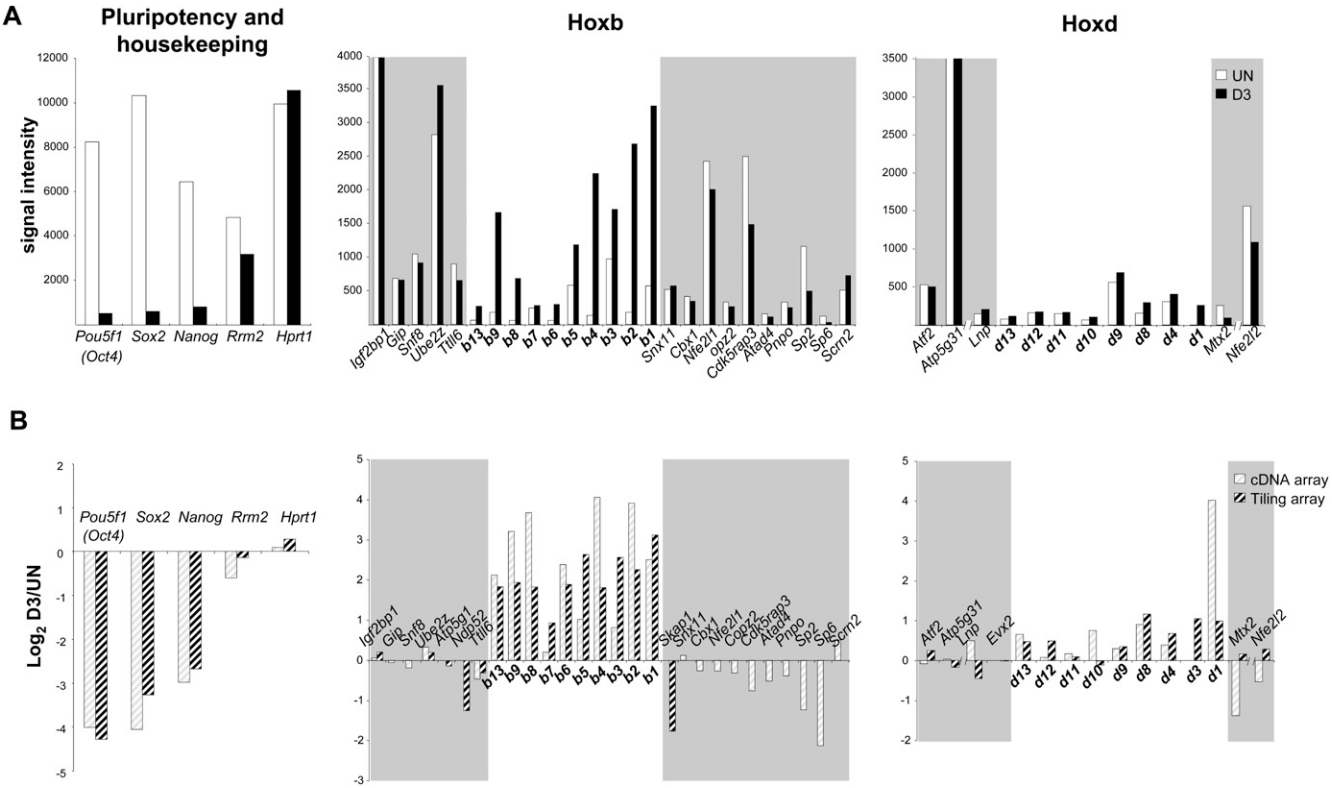

Figure 4. Gene expression around *Hoxb* and *Hoxd* during ES cell differentiation. (*A*) Signal intensities of cDNAs from undifferentiated ES cells (UN, white columns) or from cells differentiated for 3 d (D3, black columns) monitored using a cDNA microarray (GEO accession GSE15166). Results for pluripotency (*Oct4*, *Sox2*, *Nanog*) and housekeeping genes (*Rrm2*, *Hprt1*) (*left*), and the *Hoxb* (*middle*) or *Hoxd* (*right*) genomic regions are shown. (*B*) As in *A*, but showing the $\log_2$ ratio of D3/UN cDNA on a cDNA microarray (light hatched columns) or a *Hoxb*/*Hoxd* tiling microarray (dark hatched columns). Data are the mean of three independent experiments including a dye swap.

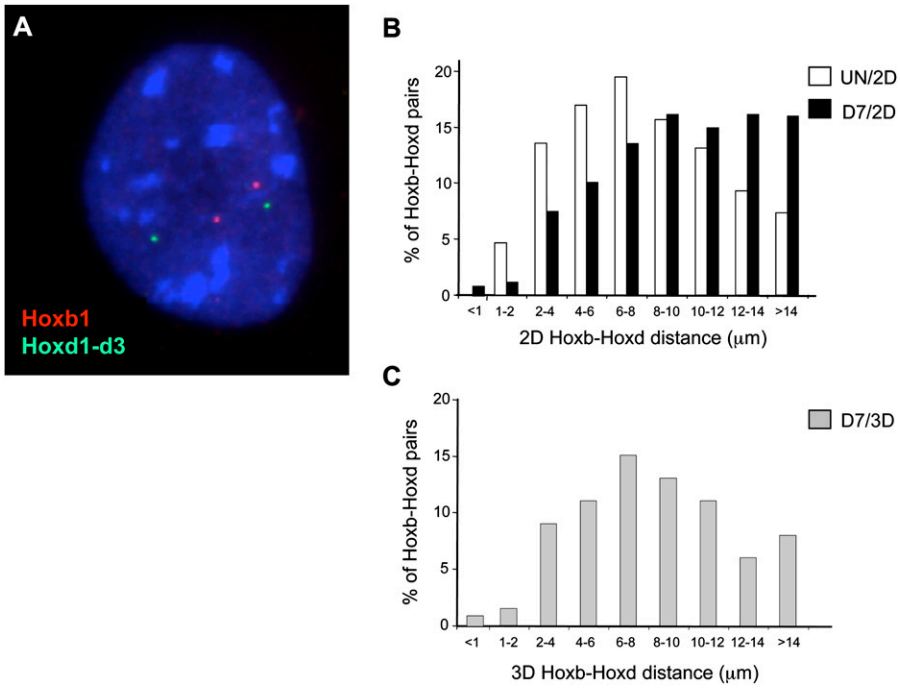

Figure 5. Spatial proximity between *Hoxb1* and *Hoxd1* loci. (*A*) Three-color DNA-FISH on DAPI counterstained nucleus from a differentiated (7 d) OS25 ES cell using probe for *Hoxb1* (BAC MMP-4; as in Chambeyron and Bickmore [2004]) in red, and fosmid probe for *Hoxd1*-d3 (WI1-121N10) in green. (*B*) Histogram showing the distribution of distances between the *Hoxb* and *Hoxd* signals measured by 2D FISH in nuclei from undifferentiated and differentiated (7 d) cells (59 and 87 nuclei analyzed, respectively). Distances are slightly larger in differentiated cells due to the increased nuclear volume. (*C*) As in *B* but using 3D FISH on pFa fixed cells.

localized outside of the CT in undifferentiated cells and this is not further increased upon differentiation (Fig. 3C). In contrast, few (8%) *Cbx1* signals were seen outside of the CT in undifferentiated cells but localization to positions exterior of the CT is increased (to >25% of alleles) during differentiation by the spread of CT reorganization emanating from *Hoxb* (Fig. 3C).

In agreement with microarray analysis, expression of *Igf2bp1* was more abundant (72% of cells showed an RNA-FISH signal) than that of *Cbx1* (27%) and this did not significantly change during differentiation (Fig. 6A). We then used DNA-FISH, with a MMU11 chromosome paint and a corresponding BAC probe, to assess the relative CT organization of transcribing vs. nontranscribing alleles in these same cells. Analysis was confined to cells where RNA-FISH signal was detectable at at least one of the alleles. Of the nontranscribing (RNA-FISH signal negative) alleles, >72% were located well inside of, and <9% were scored as exterior to, the CT in undifferentiated cells (Fig. 6B). Since RNA-FISH is likely not 100% efficient and the BACs used for DNA-FISH also encompass other neighboring genes (*Gip*, *Snf8*, *Ube2*, and *Atp5g1* for the *Igf2bp1* BAC, and *Snx11*, *Nfe2l1*, and *Copz2* for *Cbx1* BAC), we cannot exclude that some of these latter signals are actually expressing alleles of these other genes.

The distribution of actively transcribing (RNA-FISH +ve) alleles was significantly different from that of the inactive ones ($P < 0.0001$ by χ^2). Whereas, the nontranscribing alleles were preferentially located inside the CT, actively transcribing alleles were distributed between locations inside, at the edge, and outside of the CT (Fig. 6B). As the proportion of *Cbx1* alleles exterior to the CT increased during differentiation, there was no significant change in the intra-CT distribution of the nontranscribing alleles ($P > 0.05$). Therefore, it is the already active alleles that seem to be the ones that can relocate more to the outside of the CT during differentiation ($P = 0.003$).

Looping out of *Hoxb1*, but not of flanking genes, coincides with colocalization with transcription factories

Nuclear movements are thought to allow for, or to be a consequence of, recruitment of genes to specialized nuclear compartments. Actively transcribing genes have been reported to associate with foci of RNA polymerase II (RNAPII)—termed transcription factories (Osborne et al. 2004). Using immuno-DNA-FISH with an antibody (H5) specific for the Ser2 phosphorylated (elongating) form of RNAPII (RNAPIIo), we analyzed the association of *Igf2bp1*, *Cbx1*, and *Hoxb1* genomic regions with these foci (Fig. 7A). We quantified the proportion of DNA-FISH signals colocalized with, or distinct from, the foci of RNAPIIo (Fig. 7B). Approximately 30% of *Cbx1* BAC signals colocalized with RNAPIIo foci, similar to the percentage of actively transcribed *Cbx1* alleles detected in RNA-FISH. For the BAC encompassing *Igf2bp1* and neighboring genes, the percentage of colocalized loci (48%) in undifferentiated cells was lower than the proportion of *Igf2bp1* alleles with RNA-FISH signals and we do not know the reason for this. In stark contrast, there was no colocalization between *Hoxb1* alleles and RNAPIIo foci in undifferentiated cells where this *Hoxb1* is silent, but in differentiated cells 35% of alleles could now be seen to be colocalized. These data provide further support to the idea that much gene transcription takes place in association with transcription factories containing hyperphosphorylated RNAPII (Kimura et al. 2002; Osborne et al. 2004).

By comparing the spatial organization of RNAPIIo-colocalized and noncolocalized alleles, we then asked where this recruitment to RNAPII foci occurs in relation to CTs (Fig. 7C). Consistent with the RNA-FISH data (Fig. 6), *Cbx1* and *Igf2bp1* loci colocalized with RNAPIIo inside, at the edge, or outside of the CT. However, both before and after differentiation, there was a preferential distribution of the colocalized alleles away from the CT interior and toward the CT edge and exterior compared to the noncolocalized alleles ($P < 0.001$ in χ^2 test). For *Hoxb1*, there was also a preference for the associated alleles to be excluded from the interior of the CT ($P < 0.001$).

To analyze directly the association of a single transcribing gene with transcription factories, we performed RNA-immuno-FISH using intronic probes for either *Igf2bp1* or *Cbx1* on cells grown on slides, using mild conditions of fixation and permeabilization in order to preserve the nuclear architecture (Fig. 8). Greater than 60% of transcribing (RNA-FISH positive) alleles of *Igf2bp1* and *Cbx1* completely colocalized with visible foci of

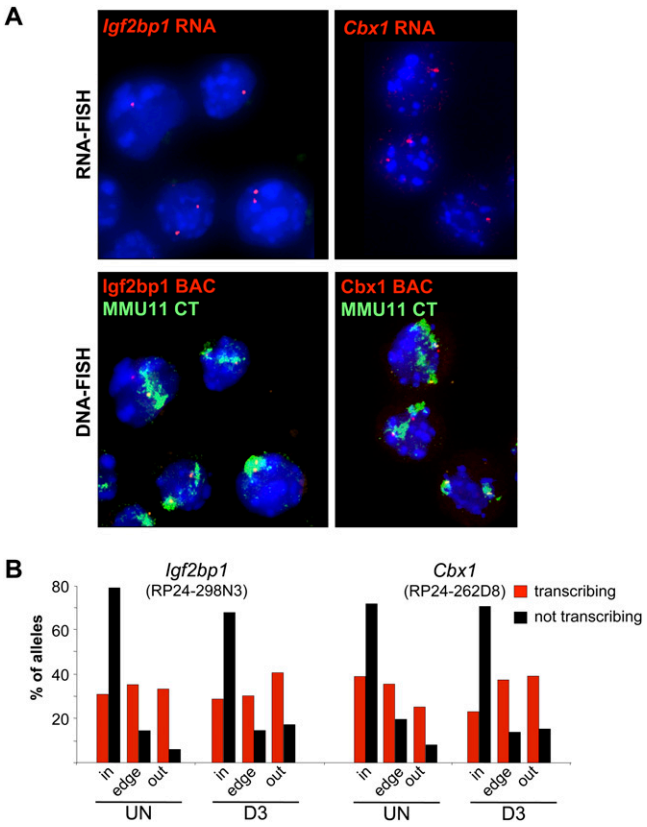

Figure 6. Nuclear organization of actively transcribing alleles. (*A*) (*Top* panels) RNA-FISH with *Igf2bp1* or *Cbx1* intronic probes (red) on DAPI counterstained nuclei of cytospun OS25 ES cells. (*Lower* panels) Same nuclei after denaturation and DNA-FISH with BAC probes overlapping *Igf2bp1* (RP24-298N3) and *Cbx1* (RP24-262D8) regions (red) together with an MMU11 chromosome paint (green). (*B*) Histogram showing the percent of actively transcribing/ RNA-FISH +ve (red) or nontranscribing (black) *Igf2bp1* or *Cbx1* alleles located inside (in), at the edge (edge), or outside (out) of the MMU11 CT in undifferentiated (UN) OS25 ES cells and in cells differentiated for 3 d (D3). Analysis was confined to cells with at least one RNA-FISH signal. For *Igf2bp1* $n = 288$ and 192, UN and D3, respectively. For *Cbx1*, $n = 320$ (UN) and 128 (D3).

RNAPIIo and <32% of RNA-FISH negative alleles were colocalized. To analyze the intra-CT position of active and inactive loci, we then denatured the nuclei and cohybridized them with a MMU11 paint and a BAC probe corresponding to either *Cbx1* or *Igf2bp1*. As expected from our previous data, we detected a differential intra-CT localization whether comparing either the RNA-FISH positive vs. negative alleles, or the RNAPIIo colocalized vs. noncolocalized alleles.

Discussion

Bystander gene activation

The clustering of genes in the genome sequence means that nuclear reorganization at one locus will inevitably influence the spatial organization of neighboring genes. If nuclear reorganization is a directed mechanism for the regulation of gene expression, then genes might be activated just because of their proximity to genes that are subject to nuclear reorganization. There are documented examples of bystander effects on gene expression (Cajiao et al. 2004; Ebisuya et al. 2008) but nothing is known about nuclear organization in these cases.

Recently, the integration of the beta-globin LCR into a region of the mouse genome containing a high density of genes with widespread and diverse expression patterns, was shown to increase the expression of some of these flanking genes in the embryonic liver—where the endogenous beta-globin locus is active (Noordermeer et al. 2008). The integrated LCR also induced both an increased localization of the region to the edge, and to the outside, of the CT, and a slightly increased association with foci of RNAPIIo. Therefore in this case, there was a bystander

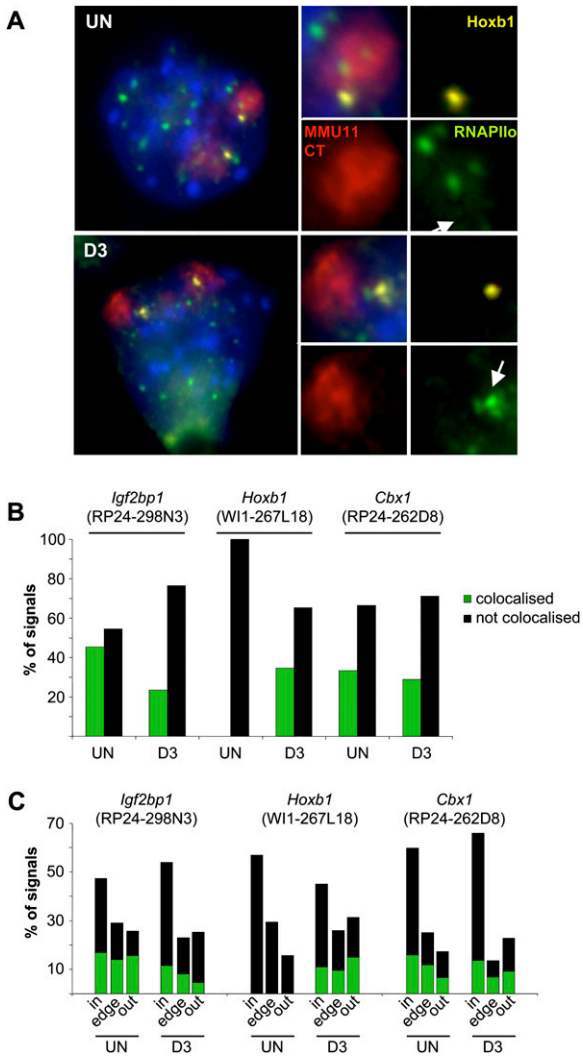

Figure 7. Locus colocalization with foci of RNAPII. (*A*) Immuno-FISH using an antibody against the phosphorylated form of RNAPII (green), *Hoxb1* probe WI1-267L18 (yellow), and MMU11 chromosome paint (red) in undifferentiated ES cells (UN) or cells differentiated for 3 d (D3). The *insets* to the *right* show magnified images from one CT with arrows indicating the position of the *Hoxb1* locus in the RNAPIIo channel. (*B*) Histogram showing the percent of signals either colocalized with (dark green) or distinct from (not colocalized; black) phosphorylated RNAPII foci for the regions encompassing *Igf2bp1* (BAC RP24-298N3), *Hoxb1* (fosmid WI1-267L18) or *Cbx1* (BAC RP24-262D8) in undifferentiated (UN) or differentiated cells (D3). (*C*) Histogram of the nuclear distribution of signals in *A* with respect to their CT edge. $n = 341$ (Un), 89 (D3) for *Igf2bp1*; 62 (Un), 73 (D3) for *Hoxb1*; and 200 (Un), 90 (D3) for *Cbx1*.

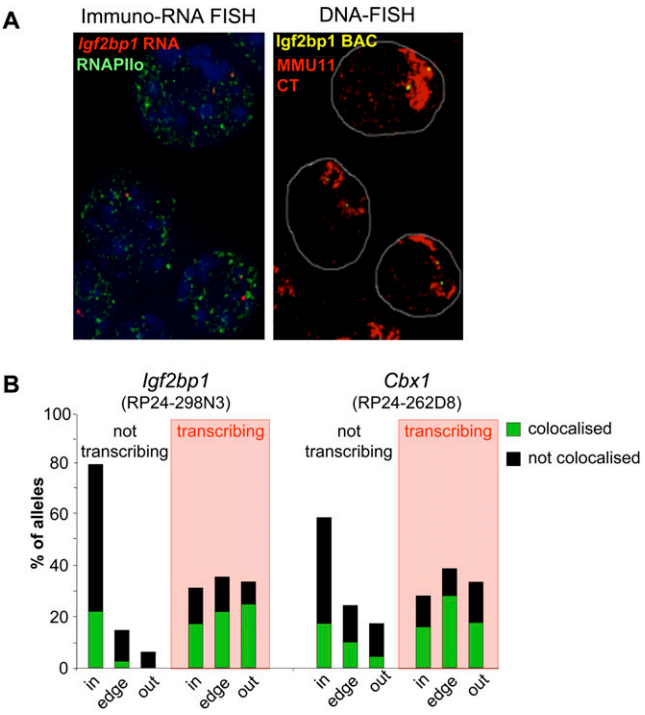

Figure 8. Active vs. inactive allele colocalization with foci of RNAPII. (*A*) Maximal projection image after deconvolution of 3D RNA-immuno-FISH using an *Igf2bp1* intronic probe (red) and an antibody against the phosphorylated form of RNAPII (green) on DAPI counterstained nuclei of undifferentiated OS25 cells (*left* panel). The DAPI channel has been attenuated in order to improve the visualization of red and green signals. The *right* panel shows the same nuclei after denaturation and DNA-FISH with a BAC probe encompassing *Igf2bp1* (RP24-298N3, yellow) together with an MMU11 chromosome paint (red). (*B*) Histogram showing the percent of nontranscribing and transcribing (shaded in red) *Igf2bp1* or *Cbx1* alleles located inside (in), at the edge (edge), or outside (out) of the MMU11 CT together with the percent of alleles colocalized with (green) or distinct from (not associated, black) a phosphorylated RNAPII focus within each category in undifferentiated OS25 cells. n = 288 (not transcribing), 206 (transcribing) for *Igf2bp1* and 128 (not transcribing), and 57 (transcribing) for *Cbx1*.

effect on both gene expression and CT organization induced by the LCR.

Here we show that there is also a bystander effect on the nuclear organization of genes flanking the 3′ side of *Hoxb*. They increase their localization to the outside of the CT during differentiation, as a consequence of *Hoxb* activation and reorganization (Fig. 3). However, there is no accompanying change in their expression (Fig. 4).

It was already known that localization outside of CTs is not sufficient to activate genes from an inactive state, but this could be attributed to lack of appropriate transcription factors (Mahy et al. 2002; Brown et al. 2006). In our study here, the *Hoxb* flanking genes are already active, but we do not observe any further increase in their expression as a result of further CT looping out. This is consistent with the conclusion of Noordermeer et al. (2008), which is that looping out is a by-product of LCR activity and that the bystander gene activation is due to direct contacts between this strong regulatory element and flanking genes. There is no known long-range regulatory element needed for *Hoxb* activation during ES cell differentiation.

Preferential localization of inactive alleles inside of chromosome territories

Even though we show that localization of *Hox* flanking genes further to the outside of CTs is not sufficient to increase their expression, we do observe a correlation between gene activity and CT organization. Using combined RNA- and DNA-FISH, we show that inactive and active alleles have a significantly different distribution within the CT from each other. Although actively transcribing alleles, as defined by the presence of a corresponding RNA-FISH signal, are found at positions inside, at the edge, and outside of the CT, inactive alleles are preferentially retained inside of the CT (Fig. 6).

Actively transcribing genes have been shown to have a preferential association with transcription factories—visibly detectable concentrations of phosphorylated RNAPII that are coincident with sites of BrUTP incorporation (Osborne et al. 2004; Brown et al. 2008). We found that the alleles of *Hoxb* flanking genes that colocalized with RNAPIIo foci were differentially localized in the CT compared to the nonassociated alleles (Fig. 7). The latter are preferentially found in the CT interior, whereas RNAPIIo colocalized alleles are distributed between positions inside, at the edge, and outside of the CT. As the frequency of alleles found outside of the CT increased during differentiation, there was no further increase in transcription factory association, consistent with the absence of increased gene expression. However, it was the alleles already associated with transcription factories, and therefore considered transcriptionally active, that seemed to be the ones that preferentially are able to be repositioned in the nucleus. Noordermeer et al. (2008) concluded that the increased transcription factory association, induced by the beta-globin LCR, occurred independent of position within the CT. However, in that study the frequency of alleles scored well inside of the CT, was too low to exclude that there may be a deficiency of factory-associated alleles in the CT interior.

Our data are consistent with previous observations of sites of BrUTP incorporation (Abranches et al. 1998; Verschure et al. 1999) or RNAPIIo concentration (Branco and Pombo 2006) within CTs. Together these data suggest that genes in the "mundane" genomic regions that flank *Hox* loci, and perhaps most genes in the genome, are transcribed in association with transcription factories (Osborne et al. 2004) that are not restricted to sites at the edge or outside of the CT. Our data do not distinguish whether genes move to preexisting factories upon activation, or whether factories might be assembled de novo upon activated genes.

We have shown here that *Hox* gene activation during the differentiation of ES cells, correlates with the association of *Hox* loci with transcription factories marked by RNAPII phosphorylated on Ser2 of the CTD. This is considered to be the actively elongating form of polymerase. The recent identification of forms of RNAPII phosphorylated on Ser5 at genes, including *Hox*, silenced by polycomb in ES cells (Stock et al. 2007), raises the possibility that in undifferentiated ES cells *Hox* loci may be associated with foci containing this form of RNAPII.

Altered chromatin mobility may explain the link between the ability to locate outside of CTs and transcription

We conclude that it is not looping out from the CT per se, but rather the ability of a genome region to be seen as looped out from the CT, that is important for active transcription. Looping out from the CT is therefore likely to be a manifestation of some other underlying change in chromatin structure that enhances

chromatin mobility (Fraser and Bickmore 2007). This might then allow genes the freedom to explore a larger proportion of the nuclear space, both inside and outside of the CT, and hence increases the probability that a gene will be able to engage with a transcription factory. In this model, it is the restraint on chromatin motion, for alleles that are not able to move outside of CTs, that restricts their ability to be transcribed and not their intra-CT position per se. This then raises the challenge of identifying the chromatin structures that modulate chromatin mobility.

Methods

ES cell culture and differentiation

OS25 ES cells were cultured as previously described (Chambeyron and Bickmore 2004; Morey et al. 2007). Differentiation was induced by plating the cells at low density without LIF or hygromycin for 1 d. Retinoic acid (RA), 5×10^{-6} M, was then added. RNA samples were collected and nuclei were prepared after 3 or 7 d of differentiation (respectively, 2 d of RA treatment and 4 d with and 2 d without RA). Similar FISH results were obtained on samples collected from two independent differentiation experiments. FISH data presented in this paper all come from the same differentiation.

Multicolor DNA fluorescence in situ hybridization

For 2D FISH, nuclei were isolated in 0.56% KCl and fixed with 3:1 v/v methanol/acetic acid (Chambeyron and Bickmore 2004). For 3D FISH, nuclei were fixed with 4% paraformaldehyde (pFa). FITC-labeled paint for MMU2 or MMU11 were purchased from CAMBIO. BAC and fosmid clones covering the *Hoxb* and *Hoxd* regions were chosen from Ensembl v37, February 2006 (http://www.ensembl.org/Mus_musculus/index.html). BAC clones were purchased from BACPAC resources center and fosmid clones were kindly provided by the Sanger Institute (for coordinates and names, see Supplemental Table S1). DNA from these clones were prepared using standard alkaline lysis and labeled with digoxigenin-11-dUTP or with biotin-16-dUTP (Roche) by nick translation. Approximately 200 ng of FITC-paint, 100 ng of biotin-labeled BAC/fosmid probe, and 100 ng of digoxigenin BAC/fosmid probe were used per slide, together with 15μg of mouse Cot-1 DNA (GIBCO BRL) and 5 μg salmon sperm DNA. Digoxigenin-labeled probes were detected using Rhodamine anti-digoxigenin and Texas red anti-sheep IgG (Vector Laboratories); biotin-labeled probes were detected using Cy5 streptavidin and biotinylated anti-avidin (Vector Laboratories) and the FITC signal from the MMU2 or MMU11 chromosome paint was amplified using F1 rabbit anti-FITC and F2 FITC anti-rabbit (CAMBIO). Hybridization, washes, detection, and imaging were as described (Chambeyron and Bickmore 2004). Slides were mounted in Vectashield (Vector) and counterstained with 0.5 μg/mL DAPI.

RNA-FISH

Probes for RNA-FISH consisted of a mix of PCR products from the introns of *Igf2bp1* or *Cbx1* and were labeled using nick translation. Primer sequences are shown in Supplemental Table S3. The RNA-FISH procedure was as previously described (Debrand et al. 1999). Briefly, cells were cytospun onto SUPERFROST glass slides (4 min, 350 rpm, Shandon Cytospin), permeabilized with 0.5% Triton X-100 in ice-cold cytoskeletal buffer complemented with 2 mM Vanadyl Ribonucleoside Complex (VRC) (New England Biolabs) for 7 min, fixed with 4% pFa on ice for 10 min and stored in 70% ethanol at 4°C. Slides were then dehydrated and hybridized directly. One microliter of RNase inhibitor (Invitrogen) was added to the hybridization mix. Hybridization conditions were the same as for DNA-FISH. Slides were washed in 50% formamide 2× SSC (pH 7.5) at room temperature, then at 37°C and then in 2× SSC at room temperature. Signal detection was as for DNA-FISH. A control with treatment with RNase confirmed signal specificity. A minimum of 50 2D images comprising at least one nucleus with an RNA-FISH signal were captured and the slide coordinates recorded. Standard DNA-FISH was then applied and the same cells relocated on the slide.

Immuno-FISH

Immunofluorescence followed by DNA-FISH was as described at http://www.epigenome-noe.net/researchtools/protocol.php?protid=3 (Chaumeil et al. 2004). Cells grown on slides were fixed with 4% pFa (pH 7.4) for 15 min at room temperature, washed twice in ice-cold PBS, and stored at 4°C in PBS. Before immunostaining, cells were permeabilized with 0.5% Triton X-100/PBS for 12 min at room temperature. Cells were then incubated with the anti-RNAPII H5 (1/100, Covance) and detected with a fluorescein anti-mouse (1/100, Vector Laboratories) secondary antibody. Slides were post-fixed with 3% formaldehyde for 10 min at room temperature, incubated in 0.1 M HCl for 10 min at room temperature, denatured for 30 min at 80°C in 50% formamide 2× SSC (pH 7.5), and hybridized.

RNA-immuno-FISH/DNA-FISH

Cells grown on slides were fixed with 3% pFA (pH 7.4) for 10 min on ice, permeabilized with 0.5% Triton X-100/PBS complemented with 2 mM VRC for 5 min on ice, washed once in 2× SSC, hybridized overnight, and washed as described above. Slides were post-fixed with 3% pFa for 10 min at room temperature and repermeabilized with 0.5% Triton X-100/PBS complemented with 2 mM VRC for 5 min on ice. Immunostaining procedure was as described above. One-one hundreths of RNase inhibitor was added to blocking buffers and primary and secondary antibodies. Three-dimensional images of nuclei with at least one RNA-FISH signal were captured and the coordinates of these cells recorded before DNA-FISH.

Image capture and analysis

Two-dimensional slides were examined using a Zeiss Axioplan II fluorescence microscope with Plan-neofluar objectives, a 100 W Hg source (Carl Zeiss) and Chroma #84000 quadruple band pass filter set (Chroma Technology Corp.) with the excitation filters installed in a motorized filter wheel (Ludl Electronic Products). Grayscale images were captured with a Hamamatsu Orca AG CCD camera (Hamamatsu Photonics Ltd.). Image capture and analysis were performed using in-house scripts written for IPLab Spectrum (Scanalytics Corp.). The distance between two probes, and probe position relative to the CT edge, were calculated as described (Chambeyron and Bickmore 2004; Chambeyron et al. 2005; Morey et al. 2007). In this analysis a probe signal is considered to be outside of the CT when its distance to the CT edge is negative. Conversely, distances >0 correspond to probe signals inside of the CT.

Three-dimensional images were captured on a Zeiss Axioplan II fluorescence microscope with the objective fitted with a Pifoc motor. Single plane images were deconvolved using the iterative restoration (20 iterations) from Volocity (Improvision) software.

Statistical analysis

The statistical relevance of DNA-FISH CT position data was assessed using the nonparametric Kolmogorov–Smirnov test to

examine the null hypothesis that two sets of data show the same distribution. The data sets consisted of at least 50 nuclei (100 territories/loci) for each differentiation time and for each combinatory of probes. A P-value < 0.05 was considered statistically significant.

The statistical significance of RNA/DNA-FISH and immuno-DNA-FISH data was assessed by χ^2.

Microarray design and hybridization

The mouse cDNA oligonucleotide microarray represented 38,000 mouse genes from the Mouse Exonic Evidence Based Oligonucleotide set (van den Ijssel et al. 2005) (GEO accession: GPL4468). For the custom tiling array, 60-mer oligos (Invitrogen/Illumina) were designed alternatively on each strand of mouse chromosome 2 and 11 to cover *Hoxd* and *Hoxb* core regions, proximal flanking regions, and distal flaking regions (one oligo every 250, 500, and 50 kb, respectively). Additional oligos were designed on exons of genes of interest: *Hoxb*, *Hoxd*, flanking genes, differentiation-related genes, and housekeeping genes (Supplemental Table S2). Amine-modified oligos were spotted at 20 μM in 1× Nexterion Spot buffer containing 0.005% Triton X100 onto Codelink activated slides by the University of Liverpool Microarray Facility.

Total RNA was extracted from OS25 cells with TriReagent (Sigma). Ten micrograms of RNA were reverse-transcribed using SuperScript Direct cDNA labeling kit (Invitrogen) to produce oligo-dT primed cDNAs labeled with Cy3 or Cy5-dCTP (Amersham). cDNAs were purified with a Qiagen PCR purification kit and quantified with a Nanodrop ND-1000 spectrophotometer. Equivalent amounts of cDNAs (1–2 μg cDNA corresponding to about 100 pmol of incorporated dye) from undifferentiated and differentiated cells labeled with a different dye were precipitated together with 10 μg of salmon sperm DNA, 500 μg of yeast tRNA and resuspended in 45 μL of hybridization buffer (50% deionized formamide, 5× SSC, 5× Denhardt, 0.1% SDS). This hybridization mix was denaturated for 8 min at 94°C and pipetted onto the prewarmed microarray slide. Hybridization was overnight under a 22 × 64 mm coverslip in a humid chamber floating in a 42°C water bath. Slides were washed with gentle shaking as follows: 2× 5 min in 2× SSC, 0.1% SDS at 42°C; 2× 5 min in 0.2× SSC at room temperature; 2× 5 min in 0.1× SSC at room temperature; and 30 s in 0.01× SSC at room temperature. Slides were dried by centrifugation at 1000 rpm, 5 min at room temperature.

Slides were scanned using Genepix (Axon Instruments). Analysis was done with BlueFuse software (Cambridge BlueGnome). Normalization between the two channels (i.e., undifferentiated/differentiated cells cDNAs) was by global Lowess for the cDNA library microarrays, and by global median based on housekeeping genes for the *Hox* tiling arrays. For the tiling arrays there were two biological and one technical (dye-swap) replicates, and for the expression arrays there were two replicates. These were normalized to each other by a Lowess normalization.

Acknowledgments

C.M. was an EMBO long-term fellow and then was a recipient of a Marie Curie Intra European Fellowship (MEIF-CT-2006-021308); C.K. was supported by the EU FP6 Network of Excellence Epigenome (LSHG-CT-2004-503433); W.A.B. is a Centennial Fellow of the James S. McDonnell foundation. We thank Bauke Ylstra (Micro Array Facility, VUMC Cancer Center Amsterdam) for the mouse expression arrays, Nick Gilbert (University of Edinburgh Cancer Research Centre) for help with *Hox* tiling microarray design, Margaret Hughes (Liverpool Microarray Facility) for microarray slide printing, and James Prendergast (MRC HGU) for Lowess normalization of data.

References

Abranches R, Beven AF, Ragon-Alcaide L, Shaw PJ. 1998. Transcription sites are not correlated with chromosome territories in wheat nuclei. *J Cell Biol* **143:** 5–12.

Bantignies F, Grimaud C, Lavrov S, Gabut M, Cavalli G. 2003. Inheritance of Polycomb-dependent chromosomal interactions in *Drosophila*. *Genes & Dev* **17:** 2406–2420.

Branco MR, Pombo A. 2006. Intermingling of chromosome territories in interphase suggests role in translocations and transcription-dependent associations. *PLoS Biol* **4:** e138. doi: 10.1371/journal.pbio.0040138.

Brown JM, Leach J, Reittie JE, Atzberger A, Lee-Prudhoe J, Wood WG, Higgs DR, Iborra FJ, Buckle VJ. 2006. Coregulated human globin genes are frequently in spatial proximity when active. *J Cell Biol* **172:** 177–187.

Brown JM, Green J, das Neves RP, Wallace HA, Smith AJ, Hughes J, Gray N, Taylor S, Wood WG, Higgs DR, et al. 2008. Association between active genes occurs at nuclear speckles and is modulated by chromatin environment. *J Cell Biol* **182:** 1083–1097.

Cajiao I, Zhang A, Yoo EJ, Cooke NE, Liebhaber SA. 2004. Bystander gene activation by a locus control region. *EMBO J* **23:** 3854–3863.

Caron H, van Schaik B, van der Mee M, Baas F, Riggins G, van Sluis P, Hermus MC, van Asperen R, Boon K, Voute PA, et al. 2001. The human transcriptome map: Clustering of highly expressed genes in chromosomal domains. *Science* **291:** 1289–1292.

Chambeyron S, Bickmore WA. 2004. Chromatin decondensation and nuclear reorganization of the *HoxB* locus upon induction of transcription. *Genes & Dev* **18:** 1119–1130.

Chambeyron S, Da Silva NR, Lawson KA, Bickmore WA. 2005. Nuclear re-organisation of the *Hoxb* complex during mouse embryonic development. *Development* **132:** 2215–2223.

Chaumeil J, Okamoto I, Heard E. 2004. X chromosome inactivation in mouse embryonic stem cells: Analysis of histone modifications and transcriptional activity using immunofluorescence and FISH. *Methods Enzymol* **376:** 405–419.

Debrand E, Chureau C, Arnaud D, Avner P, Heard E. 1999. Functional analysis of the *DXPas34* locus, a 3′ regulator of *Xist* expression. *Mol Cell Biol* **19:** 8513–8525.

Ebisuya M, Yamamoto T, Nakajima M, Nishida E. 2008. Ripples from neighbouring transcription. *Nat Cell Biol* **10:** 1106–1113.

Fedorova E, Sadoni N, Dahlsveen IK, Koch J, Kremmer E, Eick D, Paro R, Zink D. 2008. The nuclear organization of Polycomb/Trithorax group response elements in larval tissues of *Drosophila* melanogaster. *Chromosome Res* **16:** 649–673.

Ferrier DE, Minguillon C. 2003. Evolution of the *Hox/ParaHox* gene clusters. *Int J Dev Biol* **47:** 605–611.

Fraser P, Bickmore W. 2007. Nuclear organization of the genome and the potential for gene regulation. *Nature* **447:** 413–417.

Gierman, HJ, Indemans MH, Koster J, Goetze S, Seppen J, Geerts D, van Driel R, Versteeg R. 2007. Domain-wide regulation of gene expression in the human genome. *Genome Res* **17:** 1286–1295.

Kimura H, Sugaya K, Cook PR. 2002. The transcription cycle of RNA polymerase II in living cells. *J Cell Biol* **159:** 777–782.

Lanctot C, Kaspar C, Cremer T. 2007. Positioning of the mouse *Hox* gene clusters in the nuclei of developing embryos and differentiating embryoid bodies. *Exp Cell Res* **313:** 1449–1459.

Lercher MJ, Urrutia AO, Hurst LD. 2002. Clustering of housekeeping genes provides a unified model of gene order in the human genome. *Nat Genet* **31:** 180–183.

Mahy NL, Perry PE, Bickmore WA. 2002. Gene density and transcription influence the localization of chromatin outside of chromosome territories detectable by FISH. *J Cell Biol* **159:** 753–763.

Morey C, Da Silva NR, Perry P, Bickmore WA. 2007. Nuclear reorganisation and chromatin decondensation are conserved, but distinct, mechanisms linked to *Hox* gene activation. *Development* **134:** 909–919.

Morey C, Da Silva NR, Kmita M, Duboule D, Bickmore WA. 2008. Ectopic nuclear reorganisation driven by a *Hoxb1* transgene transposed into *Hoxd*. *J Cell Sci* **121:** 571–577.

Noordermeer, D, Branco MR, Splinter E, Klous P, van IJcken W, Swagemakers S, Koutsourakis M, van der Spek P, Pombo A, de Laat W. 2008. Transcription and chromatin organization of a housekeeping gene cluster containing an integrated beta-globin locus control region. *PLoS Genet* **4:** e1000016. doi: 10.1371/journal.pgen.1000016.

Osborne CS, Chakalova L, Brown KE, Carter D, Horton A, Debrand E, Goyenechea B, Mitchell JA, Lopes S, Reik W, et al. 2004. Active genes

dynamically colocalize to shared sites of ongoing transcription. *Nat Genet* **36:** 1065–1071.
Shopland LS, Johnson CV, Byron M, McNeil J, Lawrence JB. 2003. Clustering of multiple specific genes and gene-rich R-bands around SC-35 domains: Evidence for local euchromatic neighborhoods. *J Cell Biol* **162:** 981–990.
Shopland LS, Lynch CR, Peterson KA, Thornton K, Kepper N, Hase J, Stein S, Vincent S, Molloy KR, Kreth G, et al. 2006. Folding and organization of a contiguous chromosome region according to the gene distribution pattern in primary genomic sequence. *J Cell Biol* **174:** 27–38.
Simonis M, Klous P Splinter E, Moshkin Y, Willemsen R, de Wit E, van Steensel B, de Laat W. 2006. Nuclear organization of active and inactive chromatin domains uncovered by chromosome conformation capture-on-chip (4C). *Nat Genet* **38:** 1348–1354.
Singer GA, Lloyd AT, Huminiecki LB, Wolfe KH. 2005. Clusters of co-expressed genes in mammalian genomes are conserved by natural selection. *Mol Biol Evol* **22:** 767–775.
Sproul D, Gilbert N, Bickmore WA. 2005. The role of chromatin structure in regulating the expression of clustered genes. *Nat Rev Genet* **6:** 775–781.
Stock JK, Giadrossi S, Casanova M, Brookes E, Vidal M, Koseki H, Brockdorff N, Fisher AG, Pombo A. 2007. Ring1-mediated ubiquitination of H2A restrains poised RNA polymerase II at bivalent genes in mouse ES cells. *Nat Cell Biol* **9:** 1428–1435.
van den Ijssel, P, Tijssen M, Chin SF, Eijk P, Carvalho B, Hopmans E, Holstege H, Bangarusamy DK, Jonkers J, Meijer GA, et al. 2005. Human and mouse oligonucleotide-based array CGH. *Nucleic Acids Res* **33:** e192. doi: 10.1093/nar/gni191.
Verschure, P.J., van der Kraan I, Manders EM, van Driel R. 1999. Spatial relationship between transcription sites and chromosome territories. *J Cell Biol* **147:** 13–24.
Volpi EV, Chevret E, Jones T, Vatcheva R, Williamson J, Beck S, Campbell RD, Goldsworthy M, Powis SH, Ragoussis J, et al. 2000. Large-scale chromatin organization of the major histocompatibility complex and other regions of human chromosome 6 and its response to interferon in interphase nuclei. *J Cell Sci* **113:** 1565–1576.
Williams RR, Broad S, Sheer D, Ragoussis J. 2002. Subchromosomal positioning of the epidermal differentiation complex (EDC) in keratinocyte and lymphoblast interphase nuclei. *Exp Cell Res* **272:** 163–175.

Received November 9, 2008; accepted in revised form March 19, 2009.